

ALTERNATIVE METHODOLOGIES FOR EVALUATING EXPLOSION-RESISTANT MINE VENTILATION SEALS

MICHAEL J. SAPKO, ERIC S. WEISS, AND SAMUEL P. HARTEIS

*Pittsburgh Research Laboratory, National Institute for Occupational Safety and Health
Pittsburgh, PA 15236, U.S.A.*

The Pittsburgh Research Laboratory (PRL) of the National Institute for Occupational Safety and Health (NIOSH) recently conducted full-scale explosion experiments; these experiments evaluated the strength characteristics of various seal designs used for safely isolating worked-out areas in underground coal mines. Large-scale explosion tests were conducted within the multiple entry section of PRL's Lake Lynn Experimental Mine (LLEM) employing the only currently accepted test method endorsed by the Mine Safety and Health Administration (MSHA) for seal design in American mines. These explosion tests are labor-intensive, expensive to conduct, and can interfere with other critical underground safety and health research programs conducted by NIOSH. Therefore, the PRL has developed an alternative seal evaluation method, based on a hydrostatic pressure loading concept, that can facilitate the in-situ testing of seals in an operating mine. Two chambers within LLEM and one within the Safety Research Coal Mine (SRCM) were used for hydrostatic pressure loading various seal designs. The results from tests in these chambers compare favorably with those from the large-scale explosion tests in the multiple entries. Preliminary size-scaling relationships for predicting the strength of standard seal designs as a function of entry size is also presented. In addition to testing seal designs at the required 20 psi static pressure level, the new facilities also allow for the determination of the seal's ultimate failure pressure. This new approach shows promise as an alternative evaluation method for improving mine sealing technologies which, in turn, will enhance the safety of the underground personnel.

INTRODUCTION

Seals are required in U.S. ventilation plans to protect against explosions. They are used extensively in mining to isolate worked-out areas and active fire zones. Over the years, tens of thousands of seals have been erected in underground coal mines in the United

ALTERNATIVE METHODOLOGIES FOR EVALUATING EXPLOSION-RESISTANT
MINE VENTILATION SEALS

States. Seals, along with generalized rock dusting, constitute the dominant portion of America's last line of defense against underground coal mine explosions. Without reliable seals, a great number of miners' lives could be in jeopardy. During the 1990s, seven documented explosions of methane and/or coal dust occurred within sealed areas of underground U.S. coal mines (Hurren 1993; Scott et al; 1996). These explosions, believed to be initiated by lightning strikes on the surface, destroyed numerous seals and caused considerable damage in the active workings. Fortunately, these explosions did not cause fatalities or injuries. However, the potential for a disaster exists, emphasizing the need for explosion resistant seals that can perform under various mining and environmental conditions.

Title 30, Part 75.335 of the Code of Federal Regulations (CFR) states that abandoned areas of a mine must be either ventilated or isolated from active workings through the use of seals capable of withstanding a static horizontal pressure of 20 psi (138 kPa). Seals are also used to isolate fire zones or areas susceptible to spontaneous combustion. To effectively isolate areas within a mine, a seal should be designed to control the methane and air exchange between the sealed and open areas so as to prevent toxic and/or flammable gases from entering the active workings. A seal must also be capable of preventing an explosion from propagating into or out of the sealed area.

Early U.S. Bureau of Mines (USBM) research indicated that it would be unlikely for over pressures in room and pillar sealed areas to exceed 138 kPa very far from the explosion origin; provided that the area on either side of the seal contained sufficient incombustible; and gas exchange with the sealed area (Mitchell 1971.) Pressure balancing across the seals plays a key role in seal deployment strategies. This practice minimizes the exchange of gases and limits the resulting volume of flammable gas in the gob.

Many countries, including the U.S., Australia, France, Germany, Poland, South Africa, and China have pursued research for developing and evaluating explosion-resistant structures for sealing sections of underground mines. Since the early 1990s, the PRL and MSHA have jointly investigated the ability of various existing and new seal designs to meet or exceed the requirements of the CFR (Greninger et al. 1991, Weiss et al. 1993, 1996, 1997, 1999, 2002 and Sapko et al. 1999, 2001, 2003). Before any new seal design type can be deemed suitable by MSHA for use in underground coal mines, the seal design is generally required to undergo full-scale performance testing at PRL's LLEM (Triebisch and Sapko, 1990).

Figure 1 is a diagram of the seal test area in the LLEM where seal evaluation tests are conducted. Each entry contains ten data-gathering stations mounted flush to the mine rib, and each station houses a transducer to measure the static explosion pressure and an optical sensor to detect the flame arrival. All of the seals are constructed in the crosscuts

between B and C drifts. These crosscuts are approximately 2 m high by 5.8 m wide. The average cross-sectional area of the crosscuts was 11.6 m². Prior to the test, a concrete/steel bulkhead is positioned across E drift to contain the explosion pressures within C drift. For the explosion tests, methane is injected into the closed end of C drift (figure 1). A plastic diaphragm contains the methane-air mixture within the first 14 m of the drift. A fan, with an explosion-proof motor housing, mixes the methane and air. The ignition of the 9-10 % methane-air zone generates a peak pressure pulse of approximately 140 kPa as the explosion propagates down the entry. This peak static pressure pulse, measured at the wall perpendicular to the direction of propagation, remains relatively constant throughout the length of the seal test zone in C drift.

This paper provides a brief overview of the PRL's ongoing study to evaluate the use of a chamber technique for pressure loading full-size seals using compressed air, water, or confined gas explosions. Full-scale explosion testing is very elaborate, time-consuming, and costly, and often conflicts with other high-priority safety and health research conducted at the LLEM. Therefore, this effort is aimed at developing acceptable alternative methodologies to better characterize strength properties of mine seals and their ultimate interaction within the mine horizon. To this end, NIOSH constructed two test chambers within the LLEM to evaluate the equivalence of hydrostatic, pneumatic, and explosion

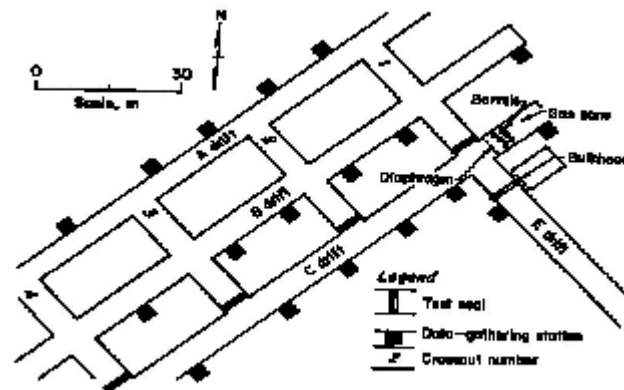


Figure 1. - Seal test area in the LLEM.

testing of seals consistent with the horizontal pressure limits specified in Title 30 CFR. The chambers allow for the determination of the ultimate failure strength of approved mine seals

and the development of geometric size scaling relationships for predicting seal performance as a function of entry cross-section.

TEST CHAMBERS

Two large-scale underground chambers were constructed within the LLEM to conduct pneumatic, hydrostatic, or explosion pressure loading of candidate seals. Figure 2 is a schematic of the large chamber. The chamber dimensions are 9.1 m wide by 4.6 m high by 3.1 m deep with a maximum cross-sectional area of 42 m². The smaller of the two chambers is 6.1 m wide by 2.4 m high by 3.1 m deep and can accommodate a seal design with a cross-sectional area up to 15 m² (Sapko et al. 1999, 2001).

Both chambers were connected via remote-controlled air valves to two diesel-driven air compressors which provide 28 m³/min (1000 cfm) of air. The air compressors were used to conduct the pre- and post-explosion leakage measurements. The air compressors were also used to slowly pressure load the seal to as high as 140 kPa, depending on the leakage rates through the seal. Via remote-controlled air valves, both chambers were connected to a 22-kw (30-hp) electric water pump capable of 6.3 L/s at 690 kPa (100 gpm at 100 psi) at the chamber inlet.

Confined explosions of methane-air within the chamber behind the seal were used to characterize the ultimate failure strength of the seal. Each chamber is equipped with a methane and oxygen injection system and an internal mixing fan for the explosion studies.

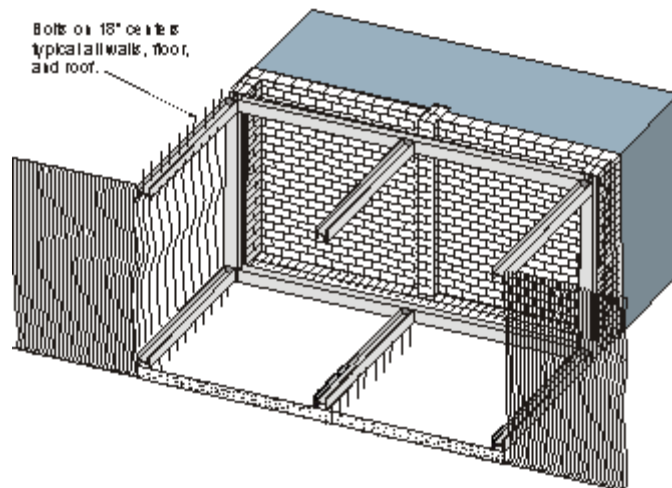


Figure 2. - Large test chamber for pressure loading of seals with water, compressed air, and with the combustion of confined concentrations of methane-air.

The oxygen and the methane are supplied by compressed gas cylinders. A pre-determined amount of 99.9% methane was metered into the chamber and thoroughly mixed with the air using a fan located within the sealed area of the chamber. The fan generates an airflow of 85 m³/min. Uniformity of pretest gas concentrations was determined by drawing gas through tubing and into an on-line infrared methane analyzer and a para-magnetic oxygen analyzer. Samples were also collected in evacuated glass tubes for subsequent analysis by gas chromatography. The flammable gas mixture was ignited at the center of the combustible volume by a 0.5-s electrical discharge from a 30-kv luminous tube transformer across a 3.2-mm spark plug gap.

The two chambers are equipped with internal 0-1.4 MPa (0-200 psia) strain gage pressure transducers (1000 Hz) for measuring the internal explosion pressure history. Three spring-loaded linear variable displacement transformers (LVDT) were mounted around a 90° bend outside the chamber and connected to the test seal via lightweight, near zero stretch polyethylene (fishing) line. This mounting system protected the expensive LVDTs from flying seal fragments. One LVDT was connected at the exact center (mid-height and mid-width) of the seal. A second LVDT was connected at the 1/4-height and mid-width point. A third LVDT was connected at the 3/4-height and mid-width point. As the seal is pressure loaded, the seal displaces outward and the LVDTs measure this displacement by generating an output signal of ~68 mv/mm. Data were recorded at 2000 samples/s per channel with a WINDAQ- PC-based data acquisition system (DAS).

Although many of the seal designs appeared to be mostly intact after the confined explosion within the chamber, some seals were later shown to be unable to properly limit the exchange of air from one side to the other. Therefore, another important factor which is considered to be part of the acceptance criteria is the ability of the seal to prevent or reduce the exchange of gases from one side of the seal to the other. The conventional method involves measuring, with an anemometer, the air that passes through the seal and a 465-cm² opening in a nearly air-tight brattice curtain installed between the seal and the anemometer, while maintaining a constant differential pressure across the seal. Measurements of the air leakages across the seals were conducted before and after the explosion tests and compared to the MSHA-established guidelines. These guidelines are as follows: for pressure differentials up to 0.25 kPa, air-leakage through the seal should not exceed 2.8 m³/min; for pressure differentials over 0.75 kPa, air leakage should be less than 7.1 m³/min. Many seal designs have withstood the required 138 kPa explosion pressure, with little visual damage, but failed the subsequent post-explosion steady-state leakage criteria.

Chamber Pre- and Post-Test Leakage

Measuring the post-test leakage from the sealed chamber is accomplished by recording the pressure decay in the chamber following the initial pressurization to 1.2 kPa (5 in H₂O) differential. The chamber, of volume V_o , is pressurized to P_1 with a gas density of ρ_1 . Mass flow rate $\dot{m} = C_w \rho v A$ occurs through an opening, where:

v = velocity of escaping gases
 \dot{m} = mass flow rate
and A = area of opening

The quantity is calculated from density change in the chamber as

$$\dot{m} = V_o \frac{d\rho}{dt}$$

At any time, t , the pressure and density in the chamber are related by an isotropic expansion relationship

$$\frac{P}{P_1} = \left(\frac{\rho}{\rho_1} \right)^\gamma$$

$$\gamma = C_p / C_v$$

$$\frac{1}{P_1} \frac{dP}{dt} = \frac{\gamma}{\rho_1^\gamma} \rho^{\gamma-1} \frac{d\rho}{dt}$$

$$\frac{d\rho}{dt} = \frac{\rho_1^\gamma}{P_1} \frac{1}{\gamma} \rho^{1-\gamma} \frac{dP}{dt}$$

but

$$\rho^{1-\gamma} = \left(\frac{P}{P_1}\right)^{\frac{1-\gamma}{\gamma}} \rho_1^{1-\gamma}$$

therefore:

$$\frac{d\rho}{dt} = \frac{\rho_1^\gamma}{P_1} \frac{1}{\gamma} \left(\frac{P}{P_1}\right)^{\frac{1-\gamma}{\gamma}} \rho_1^{1-\gamma} \frac{dP}{dt}$$

Mass flow rate through the vent is expressed by

$$\begin{aligned} \dot{m} &= -C_w V_o \frac{d\rho}{dt} \\ &= -C_w V_o \frac{\rho_1}{P_1} \frac{1}{\gamma} \left(\frac{P}{P_1}\right)^{\frac{1-\gamma}{\gamma}} \frac{dP}{dt} \end{aligned} \quad (1)$$

Experimentally, P is measured as a function of time t. This yields $\frac{dP}{dt}$ as a calculated quantity from measured P(t).

The volumetric flow through the vent vA is invariant. That is:

$$\begin{aligned} Q &= vA = \frac{\dot{m}}{\rho} \\ Q &= -\frac{1}{\rho_1} \left(\frac{P}{P_1}\right)^{-\frac{1}{\gamma}} C_w V_o \frac{\rho_1}{P_1} \frac{1}{\gamma} \left(\frac{P}{P_1}\right)^{\frac{1-\gamma}{\gamma}} \frac{dP}{dt} \end{aligned}$$

$$Q = -\frac{V_o C_w}{\gamma P} \frac{dP}{dt} \quad (2)$$

where $\gamma = 1.4$ for air
 $Q =$ volumetric loss rate from chamber, ft³
 $P =$ Chamber Pressure, inches of water gage
and $\frac{dP}{dt} =$ Decay Rate at Pressure P, in/s

Comparisons between Equation 2 and the steady-state window technique are excellent, using a discharge coefficient C_w of 1.0.

Types of Seals

Several of the seal designs evaluated previously in C Drift and in this chamber study are shown in figure 3. The standard-type, solid-concrete-block seal design was chosen for the initial evaluation since this design was extensively evaluated for several years in the PRL's Bruceton Experimental Mine (BEM) and in the LLEM. This standard-type seal was used to form the basis for the current regulations (CFR Title 30, Part 75.335). Of the solid-concrete-block seals tested in the experimental mines, only the standard-type seal design -- 406-mm-thick with staggered and fully mortared block joints, a center pilaster, floor and rib keying (hitching), and wedged at the roof (figure 3-C1) --successfully withstood the required 138 kPa pressure pulse. This same seal design was installed in both the small and large chambers.

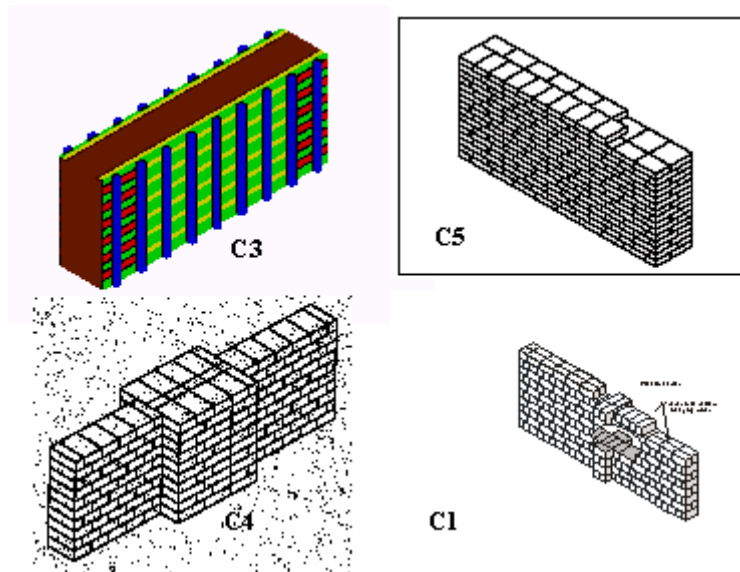


Figure 3.- Various types of seal designs tested in the new chambers. C 1 - standard-solid-block seal design; C 4 - 0.6-m thick Omega block design with 1.8-m by 1.4-m deep pilaster; C 3- 1.2-m thick plug seal design; C 5 - 1-m thick Omega block design.

Seal hitching in the chambers was accomplished by butting the seal against two 0.4-m by 0.8- m solid-concrete-block rib support columns; these columns were positioned to contact the 0.3-m-wide steel H beams. Solid-concrete-block and mortar were placed between the base of the seal and the steel H beam to simulate simple support (floor keying). Both sides of each seal were coated with a latex-based masonry waterproof sealant to help minimize air leakage during testing. Each seal was allowed to cure for 28 days before testing. Before and after each seal test, the air leakage across the seal was measured by the pressure decay technique of equation 2.

Three other seal designs deemed suitable by MSHA for use in underground U.S. mines were also selected for performance testing in the chambers. Exposing these seals to methane-air explosions within the chambers allowed for the determination of the ultimate failure pressure or approximate safety factor associated with a particular seal. Size-scaling relationships were also needed for predicting the level of pressure resistance of a seal design and/or the design thickness necessary to meet the 20 psi requirement of the CFR for entries of much larger cross-section.

Compressed Air Loading

Each seal was initially pressure loaded through the use of the twin air compressors. The air pressure behind the seal increased from 0 to 144 kPa (0-20.9 psig) in 290 s (figure 4) and then decayed to 14 kPa (2 psig) approximately 600 s after the air supply was discontinued. Due to excessive air leakage at the higher pressures and the limited capacity of the compressors, the maximum pressure obtained behind the standard-type, solid-concrete-block seal in the large chamber was 76 kPa (11 psi). For comparison, figure 4 also shows the explosion pressure history measured at a similar standard-type seal constructed within a crosscut in the multiple-entry section of the mine. The methane explosion in C drift produced a much more rapid dynamic loading of the seal but was short-lived when compared to the pressure loadings obtained from the chamber tests.

Table 1 lists results from pressure loadings of several seal designs evaluated within the chambers using compressed air. Due to excessive leakage through some seals coupled with

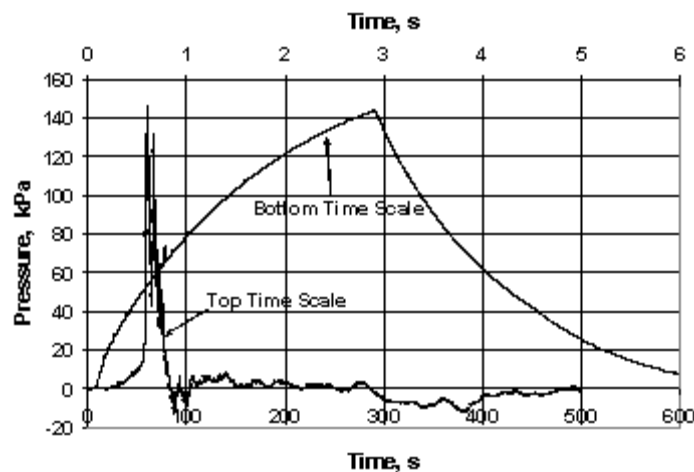


Figure 4. - Comparison of standard-type seal pressure loading at 138 kPa with compressed air in the small chamber to that of a methane-air explosion in C drift

the limited capacity of the compressors, the 138 kPa pressure load was not obtained in every test. However, through the use of hydrostatic (water) pressure loading on the chamber seals, the required pressure level was obtained every time. When considering in-situ performance testing of mine seals, the use of compressed air is more problematic and potentially dangerous for the mine personnel working in a confined area if the candidate

seal fails during the test. On the other hand, pressure loading with water is logistically simpler and safer.

Table 1 - Seal size and test results from compressed air studies

Compressed Air Chamber Tests					
Seal Test	Width, m	Height, m	Thickness, m	Max Air Pressure, kPa	Mid Seal Displacement at kPa, mm
Standard Seal					
C1-4	5.14	2.62	0.4	145	NA
L1-35	8.53	4.72	0.4	73	69 kPa-2.5 mm
¹Omega Block Seal					
C4-46	6.09	2.49	0.6	62	NA
Pumpable Plug Seal					
C3-42	6.46	2.66	1.22	190	139 kPa - 4.3 mm

Water Pressure Loading

Hydrostatic (water loading) tests were also conducted on two standard-type, solid-concrete-block seal designs. One seal, with a 5.5-m wide by 2.4-m high unsupported span between the center pilaster and each rib, was located in the small chamber within the LLEM. The other seal, having a similar 5.4-m wide by 2.4-m high unsupported span, was located in a ‘butt’ entry of the SRCM. The chambers within the LLEM are constructed in a solid unyielding limestone formation while the ‘butt’ entry in the SRCM is within the Pittsburgh coal seam.

Figure 5 is a schematic of the finished seal as constructed in the SRCM. Hitching of the seal required the removal of about 0.25-m of crushed limestone from the mine floor to expose the solid coal base. This crushed limestone was used to control water accumulations in the SRCM. A 0.15-m thick by 0.6-m wide concrete footer (approximately 21 MPa compressor strength) was constructed on the solid coal floor to provide a base for the seal. A 0.5-m wide by 0.15-m deep channel was cut vertically into both ribs to provide hitching. The small gap between the mine roof and the top of the seal was filled with

Quikcrete¹ Gunitite (16.9 ± 2.4 MPa compressive strength). Both sides of the seal were coated with a latex-based waterproofing sealant to minimize water leakage during pressure loading. The chamber behind the seal was then filled with water.

During the filling process, the displaced air within the chamber area was vented using a pipe extending through and near the top of the seal; one end of the pipe was located at the highest position within the chamber area behind the seal. When water was observed venting through the pipe, the air vent valve was closed, allowing the water pressure behind

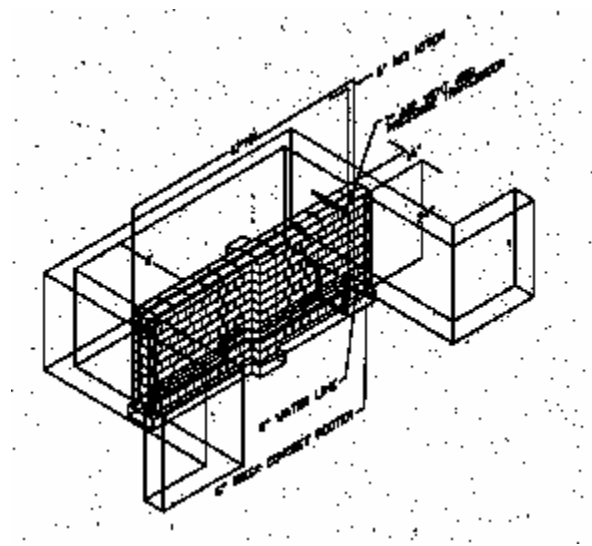


Figure 5. - Schematic of the SRCM used for water loading the standard-type seal design with pilaster.

the seal to continue to increase.

Figure 6 shows the pressure history, as recorded from a transducer located on the seal about 1.5-m above the floor, while the water flow rate was held relatively constant at 5.7 L/s (90 gpm). Then as the water displaced the air within the chamber behind the seal, the pressure began to rise. The pressure peaked at 218 kPa (31.6 psi) when the pump was stopped. The pressure then began to decay through various cracks in the mortar. After 3700 s, the 5-cm diameter pipe drain was opened.

¹Mention of product name does not imply endorsement by NIOSH.

Several tests, each with increasing water pressure loadings, were conducted on each seal design. Following each test, the water was drained and post-test air leakage

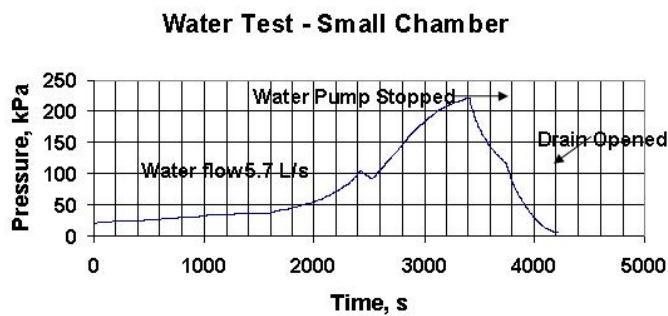


Figure 6. – Water pressure history for the standard-type seal design tested in the small LLEM chamber.

evaluations were conducted. For all cases, the post-test air leakage measurements were well within acceptable limits.

Table 2 contains the results of these water pressure tests on the standard-type, solid-concrete-block seals-- one installed in the SRCM (SRCM 1) and the other in the small chamber located within the LLEM (C6-60). Also listed in this table are the small chamber test results (C7-70) for a 1.2-m (48- in) thick pumpable plug seal. The midpoint of the standard seal in the SRCM deflected about 6 mm with a water pressure of 138 kPa, while the same design (test C6-60) deflected about 5 mm in the LLEM small chamber.

Table 2 - Seal size and test results from water pressure test

Water Pressure					
Seal Test	Width, m	Height, m	Thickness, m	Max Air Pressure, kPa	Mid Seal Displacement at kPa, mm
Standard Seal					
C6-60	5.14	2.62	0.4	221	138 kPa < 5 mm
SRCM 1	5.49	1.89	0.4	145	138 kPa -6 mm
Pumpable Plug Seal					
C7-70	6.46	2.66	1.22	173	138 kPa - 25 mm
SCRM - Safety Research Coal Mine hitched in coal seam					

Figure 7 shows the pressure history and water flow rate for the SRCM water test on the standard seal design. This test achieved a maximum flow rate of approximately 7.6 L/s (120 gpm), which produced a peak pressure of about 152 kPa (22 psi) at the roof of the chamber. Due to the hydrostatic head, the pressure at the base of the seal was about 172 kPa (25 psi).

Although in both cases (SRCM and LLEM chamber) the water capacity was insufficient to determine ultimate strength, the water capacity did generate sufficient pressures to demonstrate the seals' resistance to the required 138 kPa (20 psi) pressure loading. Additionally, the seals in both areas passed the post-test leakage criteria.

To generate sufficient water pressure behind the test seal in the chamber within the LLEM, a booster pump was used. The SRCM utilizes water originating from a local municipal water company, supplied underground through a 6-cm diameter pipe. However, for both scenarios, the water supply was insufficient to load each seal to ultimate failure. It should be noted that these water flow and pressure limitations will likely be overcome when testing in a mine environment, where hydrostatic water heads and flows are usually quite large.

For comparison to the only currently accepted test method, both the standard-type, solid-concrete-block seal and the pumpable plug seal have been previously deemed suitable by MSHA for use in underground coal mines. This suitability is based on the ability of each design to successfully withstand the 140 kPa explosion pressure pulse generated during the C drift methane ignition, while still maintaining acceptable air leakage resistance.

CHAMBER EXPLOSION TESTS

To determine the ultimate failure pressure of various seal designs that withstood the pneumatic tests within the LLEM chambers, methane-oxygen mixtures were injected into the void volume behind the seal designs and then ignited in the center of the confined

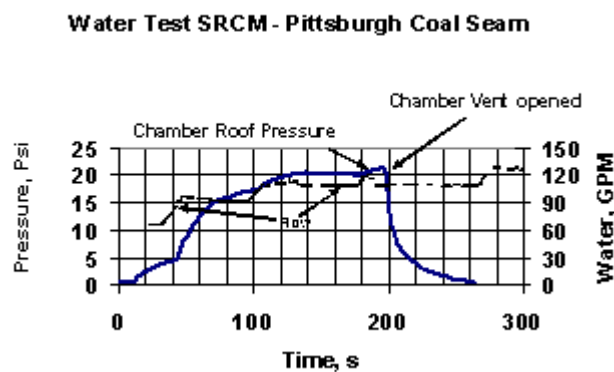


Figure 7. - Water flow and pressure loading histories for the standard-type seal design tested in the SRCM.

chamber. Obviously, this type of evaluation test using methane is intended only for controlled experimental research and not intended for use in coal mines. Several explosions of varying intensity were conducted in the small chamber against the standard-type, solid-concrete-block seal with a center pilaster (seal C1 in table 3). Four explosions were also conducted against a modified standard seal design (seal C2 in table 3) that did not include a center pilaster. In addition to the small chamber tests, a standard-type seal design with a center pilaster was tested to failure in the large chamber (seal L1 in table 3). To evaluate the size-scaling issues, this large chamber seal was constructed to the same thickness as the small chamber seal.

Table 3 - Summary of seal dimensions and explosion test results

Standard Seal*					
C1-5 ¹	5.14	2.62	0.4	390	DNR
C1-8 ¹	5.14	2.62	0.4	622	DNR
C1-9 ¹	5.14	2.62	0.4	651	DNR
C1-10 ¹	5.14	2.62	0.4	549	DNR
C1-11 ¹	5.14	2.62	0.4	688	R
C2-24	5.14	2.62	0.4	518	DNR
C2-25	5.14	2.62	0.4	524	DNR
C2-27	5.14	2.62	0.4	538	DNR
C2-29	5.14	2.62	0.4	669	R
C6-62 ¹	5.53	2.4	0.4	600	DNR
L1-35	8.53	4.72	0.4	221	R
Omega Block Seals					
C5-53	6.27	2.68	1.02	124	R
C4-48 ²	6.09	2.49	0.6	152	R
Pumpable Plug Design					
C3-44	6.46	2.66	1.22	221	R
L2	9.4	4.75	1.22	90	R
DNR - Did not Rupture R - Ruptured ¹ - Pilaster 16-in wide by 32-in deep ² - Pilaster 72-in wide by 32-in deep					

* 20 x 15 x 40 cm (nominal 8 x 6 x 16 in) solid concrete block. Average block compressive strength is 16.56 +/- 0.69 MPa (2400 +/- 100 psi)

The standard-type seal C1, withstood four constant volume explosions before it ruptured at a peak static pressure of 688 kPa (nearly 100 psi). The first four tests (C1-5, C1-8, C1-9, and C1-10 in table 3) subjected the seal to pressure loadings ranging from 390 kPa to 651 kPa (56 to 94 psi). It was only after the C1-9 test (651 kPa) that hairline cracks were visible along the central mortar joints. The post-explosion leakage rates did increase to about 2.7 m³/min (97 cfm) at 0.25 kPa (1 in H₂O), which was still within the acceptable limits. To further increase the pressure loadings for the C1-11 test, ~6 m³ (210 ft³) of oxygen was first injected into the chamber followed by the methane resulting in a near

**ALTERNATIVE METHODOLOGIES FOR EVALUATING EXPLOSION-RESISTANT
MINE VENTILATION SEALS**

stoichiometric mixture. The pressure history from the combustion of this oxygen-enriched mixture is shown in figure 8. As expected, the combustion was much more rapid as compared to the test without the oxygen injection and generated a peak static pressure of 688 kPa at 0.34 s after ignition.

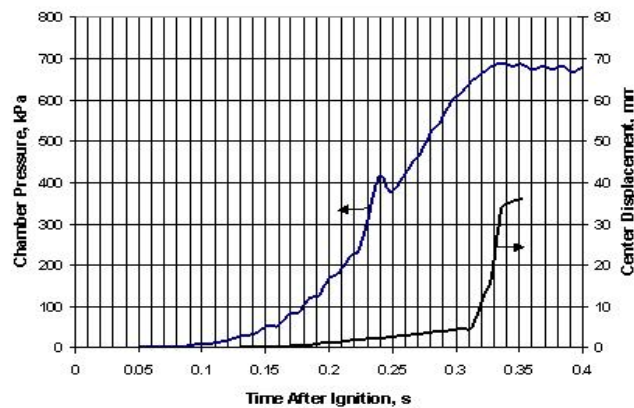


Figure 8. – Chamber pressure profile recorded during test C1-11 that resulted in the failure of the standard type seal in the small chamber.

The remains of seal C1 after rupture are shown in figure 9. The center of the seal was removed while part (152-mm thick by 406-mm wide) of the pilaster on the explosion side remains. The almost conical-shaped perimeter shear pattern is visible in the remains of the seal, indicating an arching failure pattern. As the seal deflects under load, changes in geometry cause the edges to move outward, pushing against the surrounding strata.

Shown conceptually in figure 9 are the compression zone and resultant thrust that develops from this reaction when laterally restrained. This action enhances the flexural strength of the seal at the yield lines by a compression-bending interaction. Such action significantly increases the resistance of the seal.

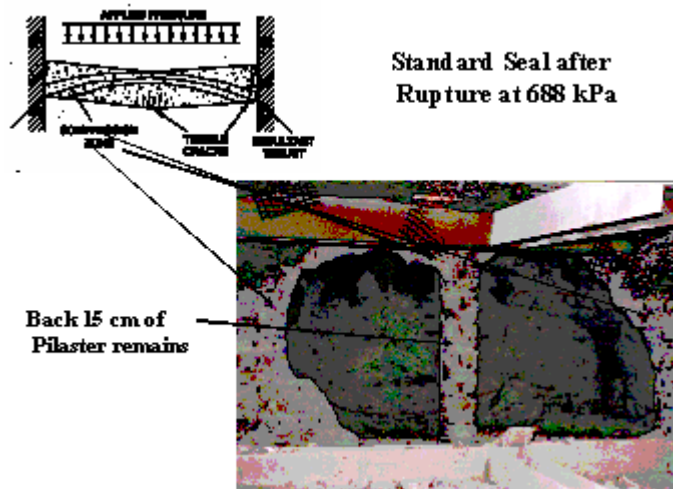


Figure 9. - Remains of the standard-type seal when exposed to 688 kPa pressure loading produced from the combustion of a methane-air-oxygen mixture.

Seal C2, without the center pilaster, ruptured during the fourth explosion at a peak static pressure of 669 kPa, or ~20 kPa below the failure pressure of seal C1 with the center pilaster. Both seals provide a margin of safety of about 4.8 to 5 times the CFR requirement.

The second series of tests was conducted in the large chamber with the standard-type, solid-concrete-block design. The main seal wall was 406 mm thick with an 813- mm thick center pilaster. Compressed air loading of the large seal to 138 kPa (20 psi) was not possible due to the leakage through and around the seal. With the two compressors operating at full capacity, the maximum attainable air pressure behind the large chamber seal was 71 kPa. At this air pressure, the LVDT indicated a maximum deflection of 2.5 mm. Post-test leakage produced an acceptable 0.7 m³/min (25 cfm) air leakage at 0.25 kPa water gauge. No visible indication of surface cracks in the horizontal or vertical mortar joints was evident. A somewhat surprising outcome of the pneumatic testing studies was that in most cases the post-test leakage was less than the pre-test leakage measurements. It appears that as the seal flexes with pressure loading, the small leakage channels seem to plug with dust or small debris as the pressure decreases and the seal relaxes.

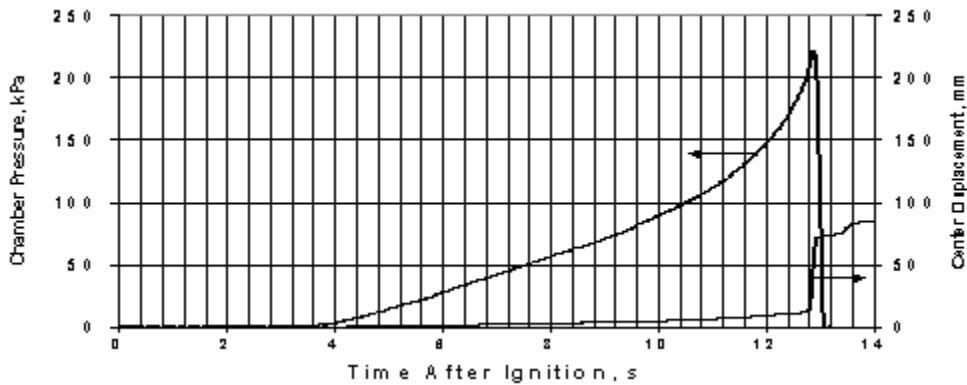


Figure 10. - Large chamber pressure recorded during test L1-35 that resulted in the failure of the standard-type seal.

After the pneumatic tests, methane was injected into the large chamber and, when mixed with the air, produced a 5.7 % methane-in-air atmosphere. The flammable gas mixture was ignited and the resulting pressure history is shown in figure 10. The chamber pressure rose rapidly to about 222 kPa in 13 seconds and then rapidly decayed to zero as the combustion gases vented through fractures, which formed as the seal began to break up and displace outward. The midpoint displacement of the seal as a function of pressure loading is shown in figure 11. The seal midpoint displaced nearly linearly (elastically) to about 12 mm and a corresponding pressure of 207 kPa (30 psig).

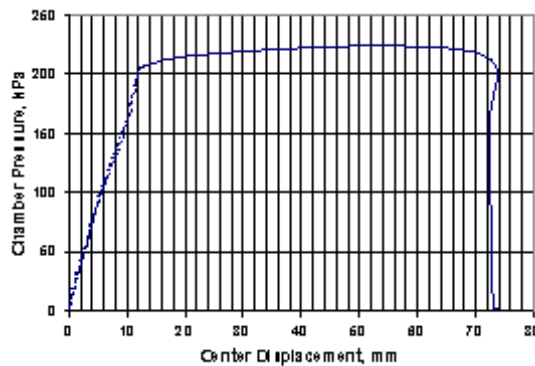


Figure 11. - Pressure loading of standard-type seal in large chamber as a function of center displacement.

As combustion continued, the chamber pressure continued to increase to about 222 kPa (32 psi) and remained relatively constant until the midpoint of the seal displaced about 71 mm-- the maximum range of the LVDT. At this point, chamber gases vented through the fractured seal and the pressure dropped to zero. These measurements indicate that the ultimate failure pressure of this seal would be between 207 and 222 kPa.

SIZE-SCALING OF SEALS

In the early 1930s (Rice et al. 1930, 1931), the USBM conducted a series of tests and found that restraining the edges of a seal caused a dramatic increase in the seal strength to a much higher level than predicted by plate theory. Full-scale explosion experiments also showed concrete walls that were recessed into the roof, ribs, and floor, and had a thickness to width ratio of at least 0.1, resisting much higher pressures than the theoretical design pressure. These results showed that recessing the ends of the concrete wall into the surrounding strata allows the wall to act as a 'flat arch'. This arching behavior transmits a lateral thrust to the strata, which then act as a buttress to prevent seal movement.

Several efforts have been made to fully understand the arching behavior through various static design models. It has been difficult to estimate structural loads due to detonations and deflagrations and the challenge of predicting load deformation behavior, especially for masonry walls. Early U.S. research on the response of walls to blast loads was conducted during World War II by the National Defense Committee (1946) then more refined methods were developed to consider the load-time history and structural parameters such as material strengths and support conditions.

The Departments of Army, Navy, and Air Force published an important document entitled "Structures to Resist the Effects of Accidental Explosions" TM 5-1300, which is useful for predicting the ultimate strength of masonry and concrete walls. As a continuation of this work, the U.S. Army Research and Development Center (Slawson, 1995) developed a single degree of freedom (SDOF) computer code to provide the engineer with a useful tool to calculate the response of typical masonry and concrete walls subjected to various blast loads. The Wall Analysis Code (WAC) calculates the resistance function (load-deflection) of a wall given construction details such as dimensions, material properties, and support conditions. The SDOF method also models the response of a structural element as a spring-mass system. The effective mass of a SDOF model is based on the deformed shape of the wall and the loading distribution. The spring stiffness describes the resistance of the responding element to deformation due to the applied loading. The resistance function may be linear, bilinear (elastic-perfectly plastic), or multi-linear. The code calculates the actual SDOF equivalent loads given the explosion pressure history and solves the equation of motion to determine the response time history of a critical central point on

the wall. The SDOF code is constrained by a height to thickness ratio of > 4 .

The WAC code was used to predict the ultimate strength of the standard seal design as tested in both the small and large chamber. The code predictions for ultimate

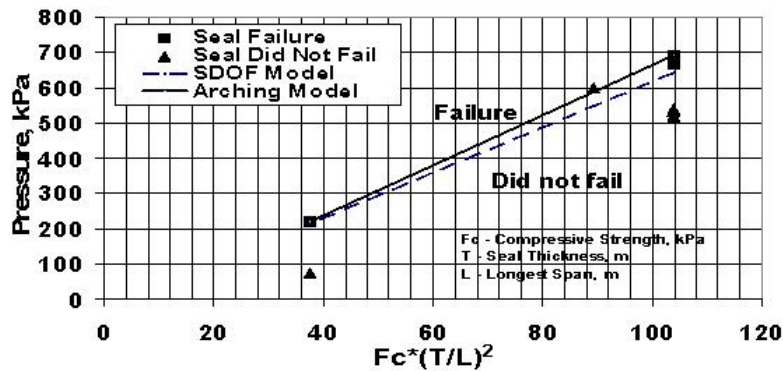


Figure 12. – Comparison of SDOF and arching model predictions for ultimate seal strength with experimental failure data for the standard-type seals in both the large and small chambers.

strength agreed well with the measured failure pressure as shown by the diamond symbol in figure 12. The straight line between the two small seals and the one large seal that failed is drawn based on the simplified formula for the arching action in transverse laterally loaded masonry wall panels (Anderson,1984) as:

$$P_{\max} = k \cdot F_c \cdot (T/L)^2$$

where P is the predicted ultimate failure pressure in kPa, F_c is the compressive strength of the block in kPa, T and L the thickness and longest span respectively of the seal in m, and k is the slope of the best fit between the seals that failed. Also shown in figure 12 are maximum chamber pressures for those tests (triangle) where the standard seal did not

rupture and passed the post-explosion leakage test. All tests except for one, which was very close, fell below the ultimate arching failure line.

The failure pressure for both the large and small standard-type seal with and without a pilaster agree well with the SDOF code predictions and the simplified arching theory:

$$P_{\max} = 6.9 * F_c * (T/L)^2$$

Although the agreement with experimental data is good, this preliminary approximation for predicting ultimate seal strength should be used with caution. The accuracy of the prediction relies on quality masonry construction, close contact between the seal and the rib abutments, and assumes that the abutment thrusts are higher than the values to cause crushing of the masonry (16.56 MPa) under arching action. These results do suggest that the arching theory approximation and the SDOF computer code predictions provide a reasonable method of approximating ultimate seal strength for seals with very rigid abutments. Research continues to refine these relationships and to develop acceptable scaling relationships for the various seal designs.

SUMMARY

Before MSHA will deem a seal design suitable for use in underground coal mines, the design has to be evaluated and, in most instances, undergo explosion testing within the LLEM. Results from this study indicate that this hydrostatic approach shows promise as an alternative method for determining the seal's performance against the 30 CFR required 138 kPa (20 psi) static pressure, more importantly, this approach is effective when the seal's actual performance is coupled with the geology of the end use mining horizon. This alternative approach using water loading in a chamber constructed within the coal seam is consistent with the intent of Title 30 CFR. Given a sufficient underground water supply, the potential exists for determining the ultimate strength of a seal design. Studies continue in these chambers to help facilitate the development of acceptable geometric size-scaling relationships for various types of seal designs. Acceptance of the in-situ water loading approach coupled with the ability to determine the ultimate failure pressure of the seal should facilitate the development and implementation of stronger seals, and thereby enhance the level of protection for underground personnel.

ACKNOWLEDGMENTS

The authors thank Charles C. Lash, technical services representative, of Burrell Mining Products International, Inc., New Kensington, PA, for providing the required labor and materials for the construction of the Omega block seal. The authors acknowledge the following Pittsburgh Research Laboratory personnel who played a key role in the experimental setup, instrumentation, and data collection activities: physical science technicians Cynthia A. Hollerich, Frank A. Karnack, Donald D. Sellers, and William A. Slivensky; electronic technicians Kenneth W. Jackson and Richard A. Thomas; and Joseph Sabo, Paul K. Stefko (foreman), and Jack M. Teatino of the SRCM. The authors also acknowledge James D. Addis, John J. Glad (lead), Timothy W. Glad, and James R. Rabon mechanical-technician contract personnel for Akima for their significant efforts in the seal construction and cleanup.

REFERENCES

- Anderson, C. Arching Action in Transverse Laterally Loaded Masonry Walls. *The Structural Engineer*, Vol 62B, No. 1, March 1984, 22 pp.
- Greninger, N. B., E. S. Weiss, S. J. Luzik, and C. R. Stephan. Evaluation of Solid-Block and Cementitious Foam Seals, USBM RI 9382, 1991, 13 pp.
- Hurren W.E., G. N. Tuggle, and F. I. McGruder. Mary Lee No. 1 Mine, Accident Investigation Report (Underground Coal Mine) U.S. Labor Dept. MSHA, August 22, 1993. Joint Departments of Army, Navy, and the Air Force, Structures to Resist the Effects of Accidental Explosions, TM 5-1300/NAVFAC P397/AFR 88-22.
- Mitchell, D. Explosion-Proof Bulkheads: Present Practices, USBM RI 7581, 1971, 16 pp. National Defense Research Committee, (1946). Effects of impact and explosions, Summary Technical Report of Division 2, Washington, D.C.
- Rice, G. S., H.P. Greenwald, H. C. Howarth, and S. Arins. Concrete Stops in Coal Mines for Resisting Explosions: Detailed Tests of Typical Stops and Strength of Coal as a Buttress. USBM Bull. 345, 1931, pp. 55-57
- Rice, G. S., H. P. Greenwald, and H. C. Howarth. Tests of the Strength of Concrete Stops Designed to Resist the Pressure of Explosions in Coal Mines, USBM RI 3036, September, 1930, 11 pp.
- Sapko, M. J., E. S. Weiss, K.L. Cashdollar, and N.B. Greninger. Overview of NIOSH's Mine Seal Research and Future Plans. The 28th International Conference of Safety in Mines Research Institutes. June 7, 1999, pp 71-85.
- Sapko MJ, Weiss ES, Trackemas JD, Stephan CR [2003]. Designs for rapid in-situ sealing. In: Proceedings of the 2003 SME Annual Meeting, Cincinnati, OH, February 24-28.
- Sapko MJ, Weiss ES, Greninger NB [1999]. Recent mine seal research conducted by

- NIOSH. Proceedings of the Sealbarr'99. Katowice, Poland, pp. 39-53.
- Sapko MJ and Weiss ES [2001]. Evaluation of new methods and facilities to test explosion-resistant seals. Proceedings of the 29th International Conference of Safety in Mines Research Institutes, Katowice, Poland, October 8-11, Vol. 1, pp. 157-166.
- Scott, D. S., E. L. Checca., C. R. Stephen, and M. J. Schultz., Oak Grove Mine, I.D. No. 01-00851, Accident Investigation Report, U.S. Labor Dept. MSHA, January 29, 1996.
- Slawson, R.T., Wall Response to Air Blast Loads: The Wall Analysis Code (WAC), U.S. Army, Engineering and Development Center, Vicksburg MS, 1995.
- Triebisch, G. and M. J. Sapko. Lake Lynn Laboratory: A State-of-the-Art Mining Research Facility, Proceedings, International Symposium on Unique Underground Structures, Denver, CO, June 12-15, 1990, CSM Press, v.2, 1990, pp. 75-1 to 75-21.
- U. S. Code of Federal Regulations. Title 30—Mineral Resources: Chapter I—Mine Safety and Health Administration, Department of Labor; Subchapter O—Coal Mine Safety and Health; Part 75—Mandatory Safety Standards—Underground Coal Mines; 1995.
- Weiss ES, Cashdollar KL, Mutton IVS, Kohli DR, Slivensky WA [1999]. Evaluation of reinforced cementitious seals. Pittsburgh, PA: U.S. Department of Health and Human Services, National Institute for Occupational Safety and Health, RI 9647.
- Weiss ES, Cashdollar KL, Sapko MJ [2002]. Evaluation of explosion-resistant seals, stoppings, and overcast for ventilation control in underground coal mining. Pittsburgh, PA: U.S. Department of Health and Human Services, National Institute for Occupational Safety and Health, RI 9659..
- Weiss, E. S., W. A. Slivensky, M. J. Schultz, C., Stephan, and K. W. Jackson. Evaluation of Polymer Construction Material and Water Trap Designs for Underground Coal Mine Seals, USBM RI 9634, 1996, 16 pp.
- Weiss ES, Slivensky WA, Schultz MJ, Stephan CR [1997]. Evaluation of water trap designs and alternative mine seal construction materials. Proceedings of the 27th International Conference of Safety in Mines Research Institutes. New Delhi, India: Oxford & IBH Publishing Company, vol. 2, pp. 973-981.
- Weiss. E.S., N. B. Greninger, C. R. Stephan, and J. R. Lipscomb. Strength Characteristics and Air-Leakage Determinations for Alternative Mine Seal Designs. USBM RI 9477, 1993, 21 pp.

LIST OF FIGURES

Figure 1. - Seal test area in the LLEM.

Figure 2. - Large test chamber for pressure loading of seals with water, compressed air, and with the combustion of confined concentrations of methane-air.

Figure 3.- Various types of seal designs tested in the new chambers. C 1 - standard-solid-block seal design; C 4 - 0.6-m thick Omega block design with 1.8-m by 1.4-m deep pilaster; C 3- 1.2-m thick plug seal design; C 5 - 1-m thick Omega block design.

Figure 4. - Comparison of standard-type seal pressure loading at 138 kPa with compressed air in the small chamber to that of a methane-air explosion in C drift.

Figure 5. - Schematic of the SRCM used for water loading the standard-type seal design with pilaster.

Figure 6. - Water pressure history for the standard-type seal design tested in the small LLEM chamber.

Figure 7. - Water flow and pressure loading histories for the standard-type seal design tested in the SCRM.

Figure 8. - Chamber pressure profile recorded during test C1-11 that resulted in the failure of the standard-type seal in the small chamber.

Figure 9. - Remains of the standard-type seal when exposed to 688 kPa pressure loading produced from the combustion of a methane-air-oxygen mixture.

Figure 10. - Large chamber pressure recorded during test L1-35 that resulted in the failure of the standard-type seal.

Figure 11. - Pressure loading of standard-type seal in large chamber as a function of center displacement.

Figure 12. - Comparison of SDOF and arching model predictions for ultimate seal strength with experimental failure data for the standard-type seals in both the large and small chambers.